Elaboration of integrated microelectrodes for the detection of antioxidant species

Céline Christophe, Fadhila Sekli-Belaidi, Jérôme Launay, Pierre Gros, Emmanuel Questel, Pierre Temple-Boyer

Elaboration of integrated microelectrodes for the detection of antioxidant species

C. Christophe[a,b,d], F. Sékli Belaidi[a,b,c], J. Launay[a,b], P. Gros[c], E. Questel[d], P. Temple-Boyer[a,b,*]

[a] CNRS, LAAS, 7 avenue du colonel Roche, F-31400 Toulouse, France
[b] Université de Toulouse, UPS, LAAS, F-31400 Toulouse, France
[c] Université de Toulouse, Laboratoire de Génie Chimique UMR CNRS 5503, Université Paul Sabatier, F-31062 Toulouse, France
[d] Pierre Fabre DermoCosmétique, Centre de Recherche sur la Peau, 31025 Toulouse, France

A B S T R A C T

(Pt–Pt–Ag/AgCl) and (Au–Pt–Ag/AgCl) electrochemical microcells (ElecCell) were developed for the detection of redox species by cyclic voltammetry. A special emphasis was placed on the SU-8 wafer-level passivation process in order to optimize the electrochemical properties of the different "thin film" metallic layers, i.e. gold or platinum for the working electrode, platinum for the counter electrode and silver/silver chloride for the reference electrode. (Au–Pt–Ag/AgCl) microcells were applied for the detection of antioxidant species such as ascorbic and uric acids in phosphate buffer solution, evidencing high sensitivity but low selectivity. Works were extended to skin analysis, demonstrating that a good electrical contact with the skin hydrolipidic film allowed the effective evaluation of the skin global antioxidant capacity.

Keywords:
Thin-film microelectrodes
SU-8 passivation
Electrochemical properties
Antioxidant species
Oxidative stress

1. Introduction

Electrochemistry provides an appropriate platform for the development of many analytical techniques in different fields including clinical biology, food industry or environment [1–5]. Indeed, electrochemical procedures provide many advantages such as easy use, low cost, fast analysis, as well as high detection sensitivity and selectivity [6]. Research works were thus dedicated to developing the electrochemical theory at a microscale level, studying bioelectrochemical sensitive layers properties and constructing micro/nanoelectrodes. Due to these works, an improvement in electroanalytical methods was achieves, consequently leading to the detection of many chemical, biochemical and biological redox species in complex media [7,8]. This is for instance the case for the evaluation of oxidative stress and the assay of specific antioxidant species on skin. Oxidative stress is known to be responsible for the production of reactive oxygen species (ROS) [9–12]. Face to pro-oxidative environments (atmosphere, pollutants, UV irradiations, pathogenic bacteria...), skin has developed different strategies to protect itself [9,13]. One of them is related to the production of hydrophilic antioxidant species such as glutathione as well as ascorbic and uric acids. As a result, concerning the skin global antioxidant capacity, the detection of these different molecules became a very important issue not only for biological researches but also for routine analysis. Recently, non-integrated ultra-microelectrodes were developed and successfully applied to the skin analysis [14–16]. Nevertheless, in order to further improve skin electrochemical analysis, microelectrodes fabrication process had to be improved in order to ensure miniaturization, mass fabrication, reproducibility, reliability and easiness of use. In order to obtain these specifications and develop integrated electrochemical microcells comprised of a three-microelectrodes system, two different technologies were proposed. Firstly, screen-printing techniques were studied for the fabrication of "thick films" electrochemical sensors [7,17]. Unfortunately, their spatial resolution is not efficient enough to reach microscale level. Secondly, technologies derived from microelectronics were developed [18]. By introducing photolithographic processes, silicon-based technologies were successfully used for mass fabrication of thin metallic micro/nanoelectrodes and integration of electrochemical microcells on different substrates (silicon, glass, polymers...) [19–23], dealing with numerous applications: chemical and biochemical detection [24–27], immunodetection [28], microfluidic electroanalysis [29–32], neurosciences [33,34],... Nevertheless, the so-fabricated thin metallic layers have still to be studied in order to control their intrinsic electrochemical characteristics and the related electrochemical microcells have to be optimized in order to be fully compatible for skin electrochemical analysis.

This paper deals with the mass fabrication of integrated, three-electrode (Pt–Pt–Ag/AgCl) and (Au–Pt–Ag/AgCl) electrochemical microcells using silicon-based microtechnologies and their application in the detection of antioxidant species. To begin with, electrochemical characteristics of different thin metallic layers, i.e.

* Corresponding author at: CNRS, LAAS, 7 avenue du colonel Roche, F-31400 Toulouse, France.
E-mail address: temple@laas.fr (P. Temple-Boyer).

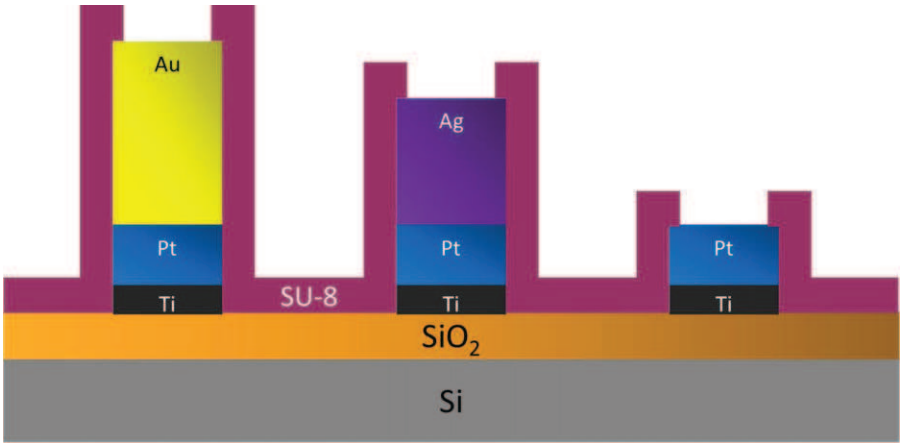

Fig. 1. Schematics of the (Au–Pt–Ag) electrochemical microcell.

gold, platinum and silver, were studied. Then, (Au–Pt–Ag/AgCl) electrochemical microcells are used for the detection of ascorbic and uric acids in various solutions. Finally, their use is extended to the skin analysis, focusing on the wafer-level passivation process improvement and examining the skin global antioxidant capacity measurement.

2. Experimental

2.1. Electrochemical microcells fabrication

(Pt–Pt–Ag/AgCl) and (Au–Pt–Ag/AgCl) electrochemical microcells (ElecCell) were fabricated on oxidized (oxide thickness: ~1 μm) silicon wafers. The different thin metallic layers were deposited by evaporation in conventional physical vapour deposition (PVD) equipments, and patterned using a bilayer lift-off process in order to improve fabrication reproducibility. Three PVD processes were performed in a row: firstly, a 200 nm platinum layer was deposited on a 20 nm titanium underlayer in order to ensure platinum adhesion on silicon oxide, followed by a 800 nm gold and a 400 nm silver layer. These different thicknesses values were chosen in order to enhance adhesion properties while limiting technological defects related to mechanical stress and inter-diffusion phenomena of metallic atoms (Ti, Pt, Au and Ag).

Finally, a biocompatible SU-8 passivation layer (thickness: 1.6 or 3 μm) was deposited at the wafer level using photolithography techniques (Fig. 1). SU-8 3005 photoresist (purchased from MicroChem Corporation) was spin-coated and a soft bake was then performed at 95 °C. The polymer crosslinking was achieved due to an ultraviolet (UV) exposure while active zones were defined using a specific photolithographic mask. A post-exposure bake was performed at 95 °C. Finally, after revealing the different metallic areas (Pt, Au, Ag) by the development of the active zones in PGMEA (propylene glycol monomethyl ether acetate), an additional UV exposure and a final hard-bake were conducted to ensure the SU-8 layer complete polymerization. This wafer-level passivation process was used to insulate electrically the different metallic layers and define precisely the different active surfaces. The gold or platinum working microelectrodes were defined as disks and their electroactive area was approximately 4.9×10^{-4} mm^2 (diameter: 25 μm). In contrast, very large silver/silver chloride reference microelectrode (0.02 mm^2) and platinum counter microelectrode (1 mm^2) were fabricated. (Pt–Pt–Ag) and (Au–Pt–Ag) electrochemical microdevices were manufactured on silicon chip (Fig. 2). The whole chip was then placed and glued by an epoxy insulating glue on a specifically coated printed circuit, wire bonded and packaged at the system level using a silicone glop-top in order to be fully compatible with liquid phase measurement (Fig. 2). For each microdevice, the silver/silver chloride Ag/AgCl reference was finally obtained by oxidizing the silver metallic layer in a 0.01 M KCl solution. This oxidation was performed by linear voltammetry (potential scan rate: 1 mV s^{-1} between 0.1 and 0.25 V/SCE) using a standard saturated calomel electrode (SCE) $Hg/Hg_2Cl_2/KCl_{sat}$ as reference.

2.2. Electrochemical microcells characterization

All the electrochemical characterizations were held using a multi-channel VMP potentiostat from Biologic. Surfaces of the "thin film" platinum and gold working microelectrodes were electrochemically characterized by cyclic voltammetry in a deaerated 0.5 M H_2SO_4 solution (potential scan rate: 50 mV s^{-1} between −0.25 and +1.2 V/SCE, and between −0.3 and +1.6 V/SCE respectively). Their active surface was then evaluated by plotting a current–potential curve (potential scan rate: 50 mV s^{-1} between −0.5 and +0.3 V/SCE) in a deaerated, 0.1 M, pH 7.0 phosphate buffer

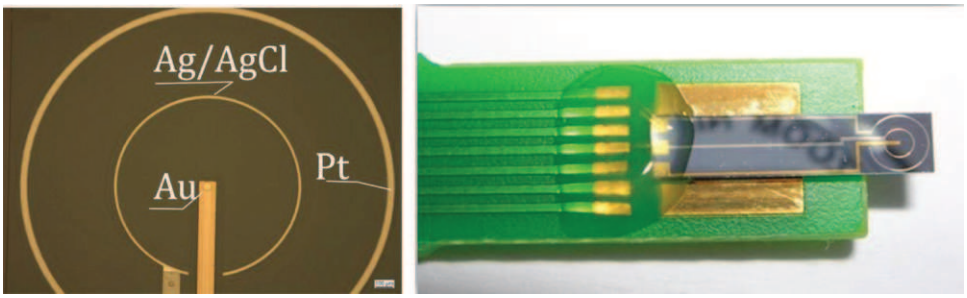

Fig. 2. Details of the (Au–Pt–Ag) electrochemical microcell chip and realisation of the (Au–Pt–Ag/AgCl) ElecCell microsensor.

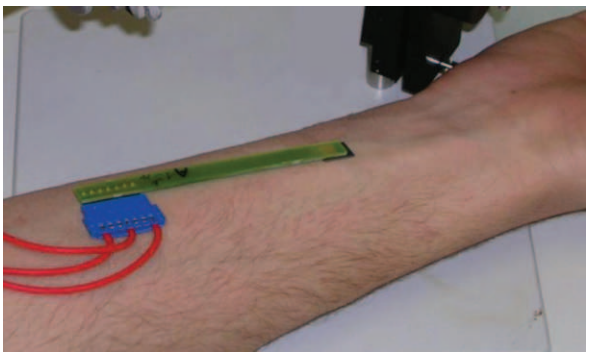

Fig. 3. Use of the (Au–Pt–Ag/AgCl) electrochemical microcell for the skin analysis.

solution (PBS) containing 0.005 M of ferricyanide ions $Fe(CN)_6^{3-}$. Considering a steady-state regime, the microelectrode radius was calculated according to the Saïto relation [35]:

$$I_{lim} = 4nFDCr \quad (1)$$

where F is the Faraday constant ($F = 96500\ C\ mol^{-1}$), n is the number of electrons exchanged per mole ($n = 1$), and C and D are the $Fe(CN)_6^{3-}$ ion concentration and diffusion coefficient, being estimated to 5×10^{-3} mol L^{-1} and $7 \times 10^{-6}\ cm^2\ s^{-1}$ respectively [36,37].

The electrochemical characteristics of the "thin-film" silver microelectrodes were studied by cyclic voltammetry in a deaerated 0.1 M KNO_3 acid (pH 3.5) solution (potential scan rate: 50 mV s^{-1} between −1 and +0.5 V/SCE). Finally, the efficiency and stability of the resulting Ag/AgCl reference microelectrode were evaluated by monitoring the Nernst potential at equilibrium in a 0.01 KCl solution and compared with a standard saturated calomel electrode (SCE).

All the chemical reagents were purchased from Sigma.

2.3. Electrochemical characterization of antioxidant species in solution and on the skin

The whole (Au–Pt–Ag/AgCl) ElecCell microsensors were tested in an autonomous way, i.e. using the "three integrated microelectrodes" configuration, for the detection of two antioxidant molecules: ascorbic (AA) and uric (UA) acids. This was performed by cyclic voltammetry (potential scan rate: 50 mV s^{-1} between −0.2 and +0.8 V) in a PBS pH 7.0 containing ascorbic acid and/or uric acid (concentration: 10^{-3} M, purchased from Sigma). Their analytical performances were compared with standard "non-integrated" gold microelectrode presented in previous papers [14,16]. For a better comparison of the different amperometric responses, the residual voltammogramms obtained in PBS were deduced from those obtained with AA and/or UA species.

Finally, electrochemical characterization of antioxidant molecules was extended to skin analysis by applying directly the (Au–Pt–Ag/AgCl) ElecCell microsensors on the forearm skin surface (Fig. 3).

3. Results and discussion

3.1. Electrochemical characteristics of the platinum thin film

(Pt–Pt–Ag/AgCl) electrochemical microcells were first characterized by cyclic voltammetry. Fig. 4 shows the cyclic voltammogram typically obtained with the "thin film" platinum working microelectrode (SU-8 thickness: 1.6 μm) in a 0.5 M deaerated H_2SO_4 solution. The curve shape is representative of polycrystalline platinum [38–40]: the oxidation and reduction

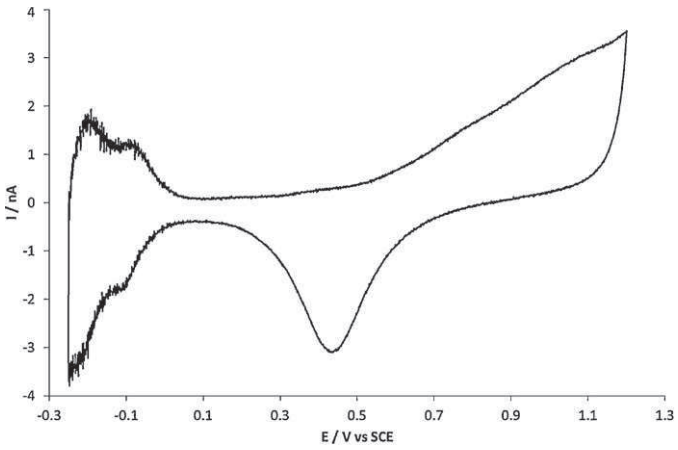

Fig. 4. Cyclic voltammogram obtained with the "thin film" platinum working electrode (SU-8 thickness: 1.6 μm) in a deaerated 0.5 M H_2SO_4 solution (potential scan rate: 50 mV s^{-1}).

peaks related to the PtH_2 and PtH species appeared in a potential range between −0.25 and 0 V. The platinum oxidation began around 0.6 V and the solvent oxidation was around 1.2 V. The peak potential corresponding to the reduction of the platinum oxides previously obtained at the electrode surface was found around 0.45 V.

Cyclic voltammograms recorded with the "thin film" platinum working microelectrode in a deaerated 0.005 M $Fe(CN)_6^{3-}$ solution yielded a steady-state diffusion-limited current even without stirring the solution and with a relatively high potential scan rate of 50 mV s^{-1} (figure not shown). According to Eq. (1), the I_{lim} experimental value was approximately 34 nA current. This value corresponded to an electroactive surface of approximately 5×10^{-4} mm^2, i.e. to a radius around 25 μm, which was agreement with the working microelectrode dimension.

In conclusion, the "thin film" platinum layer exhibited electrochemical properties similar to those usually demonstrated on solid platinum as well as well-defined electroactive area.

3.2. Electrochemical characteristics of the gold thin film

Similar experiments were performed for the (Au–Pt–Ag/AgCl) electrochemical microcells and the associated "thin film" gold microelectrode. Fig. 5 shows successive cyclic voltammograms recorded in a deaerated 0.5 M H_2SO_4 solution for a 1.6 μm-thick SU-8 passivation layer. The curves demonstrated that the gold

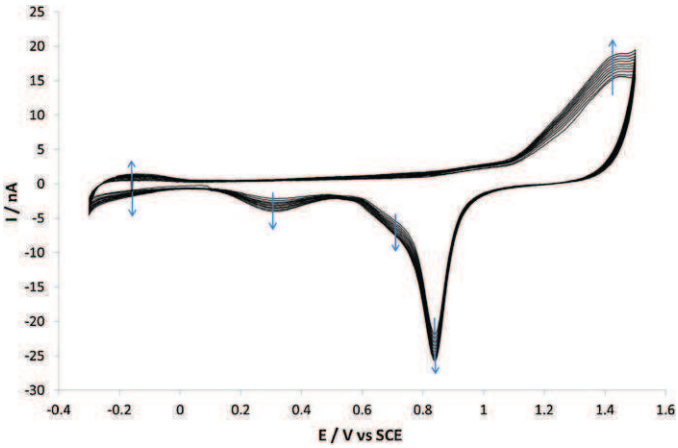

Fig. 5. Cyclic voltammograms obtained with the "thin film" gold working electrode (SU-8 thickness: 1.6 μm) in a deaerated 0.5 M H_2SO_4 solution (potential scan rate: 50 mV s^{-1}). Arrows indicate the curve evolutions with time.

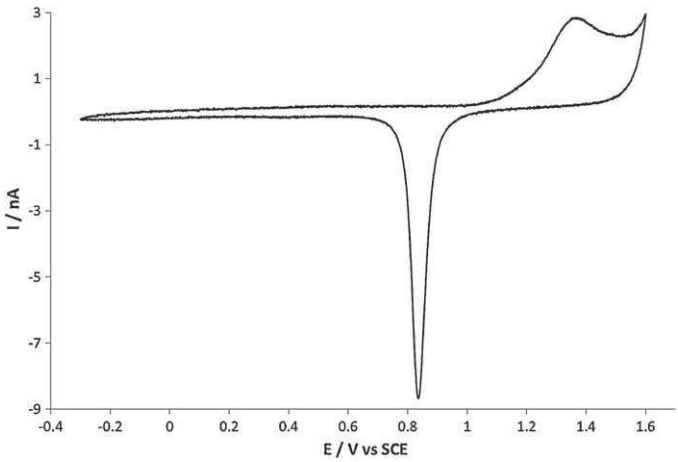

Fig. 6. Cyclic voltammograms obtained with the "thin film" gold working electrode (SU-8 thickness: 3 μm) in a deaerated 0.5 M H_2SO_4 solution (potential scan rate: 50 mV s^{-1}).

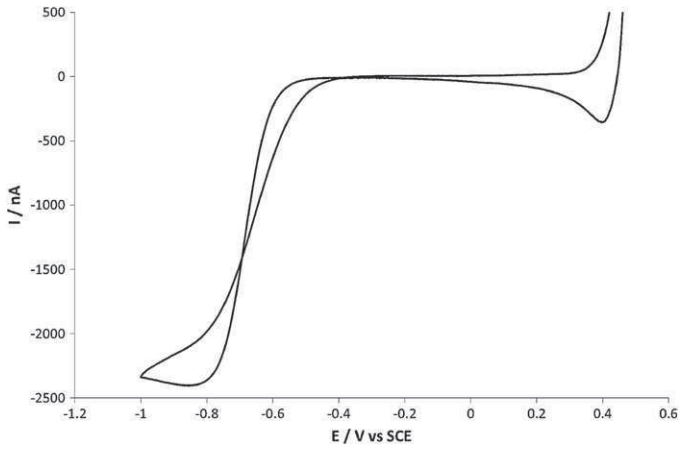

Fig. 7. Cyclic voltammogram of the "thin film" silver electrode (SU-8 thickness: 3 μm) in a deaerated 0.1 M KNO_3 solution (potential scan rate: 50 mV s^{-1}).

oxidation wave began at 1 V and that peak corresponding to gold oxides reduction appeared close to 0.85 V [41,42]. Nevertheless, some other amperometric signals are also observed at −0.2 and 1.3 V in the anodic part of the curve as well as at 0.3 and −0.2 V during the cathodic scan. All these signals increased with the number of potential cycles (see evolution arrows on Fig. 5). Since these unexpected curves were not evidenced for the "thin-film" platinum microelectrode (see Section 3.1), they can be attributed to the Au/SU-8 interface phenomena. On the one hand, non-adhesion of the SU-8 film on gold as well as poor step coverage due to the Ti/Pt/Au stacking higher thickness (∼1000 nm rather than ∼200 nm for the Ti/Pt one) is responsible to passivation defects, allowing the titanium/platinum underlayer to be in contact with the electrolytic solution [43]. On the other hand, the sulphur-based triarisulfonium salts of the SU-8 resin are electrochemically active on the gold surface [44]. This was confirmed by cyclic voltammetry performed on SU-8/cyclopentanone solutions (figure not shown).

In order to reduce both redox phenomena, two developments were proposed. Firstly, the SU-8 polymerization process was optimized in terms of exposure dose and annealing duration to counteract any electrochemical interference. Secondly, the SU-8 thickness was increased from 1.6 to 3 μm to improve step coverage and avoid any contact between the metallic underlayers and the electrolytic solution. Fig. 6 shows the resulting cyclic voltammogram in the same deaerated 0.5 M H_2SO_4 solution. The curve was very similar to that typically recorded with solid gold while the current peaks corresponding to the oxidation of gold and the reduction of gold oxides were only observed in this case. Compared to Fig. 5, lower current levels were evidenced, demonstrating that a better control of the gold microelectrode electrochemical active area was obtained. This was confirmed by characterizing by cyclic voltammetry these optimised "thin film" gold working microelectrodes in a deaerated 0.005 M $Fe(CN)_6^{3-}$ solution (result not shown). Similarly to the "thin film" platinum microelectrode (Section 3.1), a steady-state diffusion-limited current of 32 nA was recorded. As expected, according to Eq. (1), the working electrode electroactive surface and radius were estimated to 4.3×10^{-4} mm^2 and 23.5 μm respectively.

So, by improving the SU-8 polymerisation process and by increasing the SU-8 passivation thickness from 1.6 to 3 μm, "thin film" gold working microelectrodes with good electrochemical properties and well-defined active area, were successfully obtained. Finally, it should be mentioned that the increase in SU-8 thickness from 1.6 to 3 micrometers did not induce any degradation of the "thin film" platinum working microelectrodes (cf. Section 3.1).

3.3. Study of the Ag/AgCl reference microelectrode

Cyclic voltammograms typically obtained with the "thin-film" silver microelectrodes (SU-8 passivation thickness: 3 μm) were recorded in a deaerated 0.1 M KNO_3 acid (pH 3.5) solution (Fig. 7). Typical curves were obtained: the silver oxidation starts around 0.3 V, the associated reduction was clearly shown around 0.4 V and the final proton reduction is evidenced under −0.5 V.

Finally, the temporal stability of the "thin film" Ag/AgCl reference microelectrode was studied by measuring its potential using the SCE reference electrode in a 0.01 KCl solution for a 10 min duration. The Ag/AgCl microelectrode potential at equilibrium was found to be quite stable around 0.1225 V (result not shown). This value is higher than the theoretical one given by the Nernst law, i.e. 0.098 V. Such discrepancy was related to AgCl layer defects and to chemical activities of chloride ions Cl^- and/or Ag-related species [45,46]. Nevertheless, after an initial decrease around 0.5 mV during 1 min, the potential drift of the Ag/AgCl integrated electrode was very low (around 1 μV s^{-1}), in agreement with literature [46].

3.4. Detection of antioxidant species

(Au–Pt–Ag/AgCl) electrochemical microcells (SU-8 passivation layer thickness: 3 μm) were applied for the detection of antioxidant molecules, and more precisely ascorbic and uric acids (AA and UA), in pH 7.0 phosphate buffer solution (PBS). All the cyclic voltammograms were obtained in an autonomous way, i.e. using the "three integrated microelectrodes" configuration. In all cases, no significant signal was observed in PBS pH 7.0 except for the gold oxidation starting around 0.8 V. This PBS-related residual voltammogram was systematically deduced from that obtained with antioxidant molecules in order to improve results analysis.

The ElecCell microsensor was first used for the detection of ascorbic acid (AA – 0.001 M) and uric acid (UA – 0.001 M) separately (Figs. 8 and 9). In both cases, cyclic voltammograms evidence an oxidation wave starting around 0 V for the AA solution and around 0.3 V for the UA one [47,48]. Compared to the solid gold microelectrode and whatever the antioxidant species, the ElecCell microsensor responses showed similar half-wave potential $E_{1/2}$ and higher diffusion current density i_{lim}, i.e. thus providing higher sensitivity (Table 1). Such enhancement should be related to the electrocatalytic properties of solid gold electrode and thin metallic layer deposited by PVD, respectively and could result from change

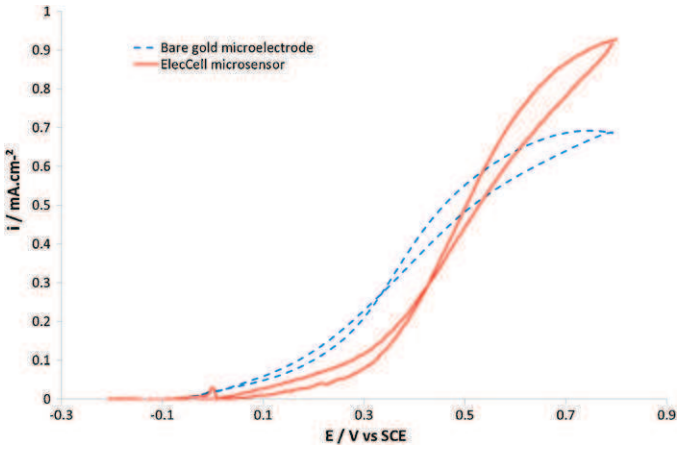

Fig. 8. Cyclic voltammogram of the (Au–Pt–Ag/AgCl) electrochemical microcell (solid line) and of the standard "non integrated" gold electrode (dotted line) in a PBS pH 7.0 solution containing AA 0.001 M (potential scan rate: 50 mV s^{-1}).

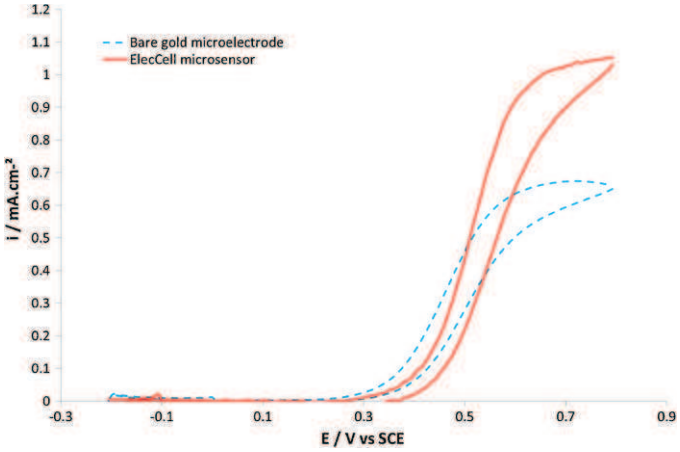

Fig. 9. Cyclic voltammogram of the (Au–Pt–Ag/AgCl) electrochemical microcell (solid line) and of the standard "non integrated" gold electrode (dotted line) in a PBS pH 7.0 solution containing UA 0.001 M (potential scan rate: 50 mV s^{-1}).

in crystallographic orientation or surface roughness. Anyway, the use of (Au–Pt–Ag/AgCl) ElecCell microsensors for the detection of ascorbic and/or uric acids in liquid phase was successfully demonstrated.

Finally, the ElecCell microsensor was studied in phosphate buffer solution containing both ascorbic and uric acids (AA + UA – 0.001 M (Fig. 10). As expected and similarly to that obtained with the standard "non integrated" gold electrode, cyclic voltammograms evidenced two oxidation waves related to the two antioxidant species. As before, slightly higher diffusion current I_{lim}, and therefore higher detection sensitivity, were obtained with the ElecCell microsensor, resulting in higher sensitivity (Table 1). Nevertheless, these waves are not clearly defined and are therefore difficult to separate. Half-wave potential $E_{1/2}$ were roughly defined, leading to low detection selectivity between ascorbic and uric acids [49,50]. This problem could be solved by developing

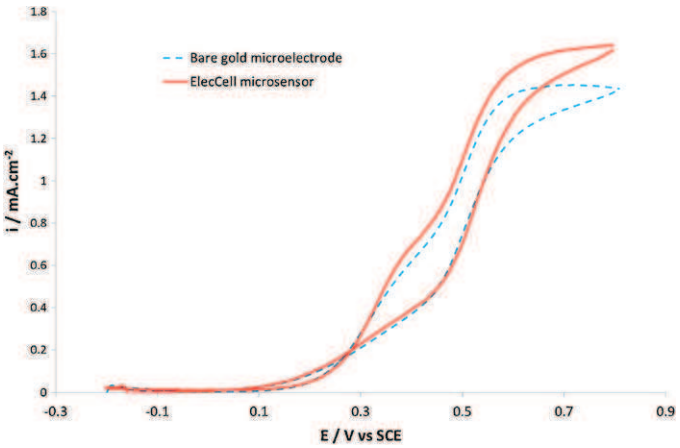

Fig. 10. Cyclic voltammogram of the (Au–Pt–Ag/AgCl) electrochemical microcell (solid line) and of the standard "non integrated" gold electrode (dotted line) in a PBS pH 7.0 solution containing AA and UA 0.001 M (potential scan rate: 50 mV s^{-1}).

specified functionalization based on electroactive polymers such as poly(3,4-ethylenedioxythiophene) (PEDOT) [16]. Works are in progress in this way.

3.5. Skin analysis for the antioxidant capacity measurement

The (Au–Pt–Ag/AgCl) electrochemical microcells were finally tested for skin analysis in order to determine the global antioxidant capacity detection feasibility. The experimental protocol was quite simple since the ElecCell microdevices were applied directly on the forearm without any pre-treatment (Fig. 3). The main principle was to use the "stratum corneum" natural hydrolipidic film to guarantee the electrical contact between the working, counter and reference microelectrodes [51].

Logically, the ElecCell microsensors with a 3 μm-thick SU-8 passivation layer were first studied. In this case, no amperometric signal was evidenced on the skin while performing cyclic voltammetry experiment. However, as soon as few pH 7.0 phosphate buffer solution (PBS) droplets were deposited on the skin surface, the typical gold voltammogram was found again. Such result demonstrates that the hydrolipidic film was not sufficient to provide the electrical contact between the different microelectrodes since its thickness is known to be around one micron [51,52].

In order to tackle off this bottleneck and to improve the electrical contact on the skin surface, the microelectrodes recess and therefore the SU-8 layer thickness must be decreased. So, even if their electrochemical performances were lower, the ElecCell microsensors with a 1.6 μm-thick SU-8 passivation layer were also used for the skin analysis using cyclic voltammetry (Fig. 11). In this case, thanks to the passivation thickness decrease, a good electrical contact was obtained with the hydrolipidic film. Furthermore, no electrochemical interference was evidenced (cf. Section 3.2). This improved electrical behaviour was related to the hydrolipidic film physical properties. Compared to water-based solutions, this emulsion-like, two-dimensional medium is characterized by a higher viscosity, lower diffusivities and a higher electrical resistivity [51,52]. Thus, obtained voltammograms were typical of the

Table 1
Characteristics of the (Au–Pt–Ag/AgCl) electrochemical microsensor responses for the detection of ascorbic and/or uric acids.

		Ascorbic acid (AA)	Uric acid (UA)	Ascorbic and uric acids (AA + UA)
ElecCell microsensor	$E_{1/2}$ (V/SCE)	0.47 ± 0.08	0.51 ± 0.03	0.31 ± 0.03/0.53 ± 0.01
	i_{lim} (mA cm^{-2})	0.9 ± 0.1	1.1 ± 0.3	0.69 ± 0.04/0.91 ± 0.07
Standard gold electrode	$E_{1/2}$ (V/SCE)	0.35 ± 0.02	0.48 ± 0.02	0.31 ± 0.03/0.52 ± 0.02
	i_{lim} (mA cm^{-2})	0.73 ± 0.08	0.67 ± 0.05	0.6 ± 0.05/0.81 ± 0.07

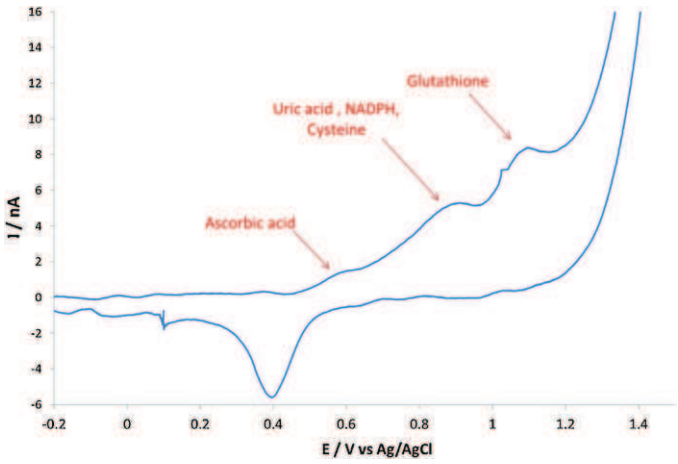

Fig. 11. Cyclic voltammogram of the (Au–Pt–Ag/AgCl) electrochemical microcell on the skin surface (potential scan rate: 50 mV s^{-1}).

electrochemical skin properties [14,53]. The ascorbic acid oxidation was responsible for the first current wave around 0.6 V/SCE. Then, the second wave around 0.8 V/SCE was related to uric acid, nicotinamide adenine dinucleotide phosphate (NADPH) and cystein. The last wave around 1.2 V/SCE was associated to the glutathione oxidation. Finally, the reduction peak observed around 0.4 V/SCE was due to the gold oxides.

All in all, by decreasing the SU-8 layer thickness and therefore the microelectrodes recess to 1.6 μm, the skin hydrolipidic film was sufficient to obtain a good electrical contact between the different microelectrodes and to detect electrochemically different antioxidant species present on the skin surface.

4. Conclusion

(Pt–Pt–Ag/AgCl) and (Au–Pt–Ag/AgCl) electrochemical microcells (ElecCell) were fabricated using silicon-based technologies derived from microelectronics in order to detect redox species, and more specifically antioxidant molecules such as ascorbic and/or uric acids in liquid phase. What is more, electrochemical analysis for the skin global antioxidant capacity measurement was performed. Specific emphasis was placed on the SU-8 wafer-level passivation process. In order to optimize the electrochemical properties of the different "thin film" metallic layers, i.e. gold for the working electrode, platinum for the counter electrode and silver/silver chloride for the reference electrode, it was necessary to increase the SU-8 layer thickness up to 3 μm. Thus, the ElecCell microsensors were studied for the detection of ascorbic and uric acids in phosphate buffer solution. Compared to standard "non integrated" gold electrodes, similar responses were shown by cyclic voltammetry, evidencing higher detection sensitivity but low detection selectivity.

Works were extended to skin analysis. In this case, the 3 μm-thick SU-8 layer was responsible for a very high microelectrode recess to provide a good electrical contact with the skin hydrolipidic film. However, using a non-optimized 1.6 μm-thick SU-8 layer, oxidation waves related to different antioxidant species were successfully obtained on the skin, demonstrating that the stratum corneum global antioxidant capacity can be effectively measured.

In order to use (Au–Pt–Ag/AgCl) ElecCell microsensors for the skin analysis, a compromise has to be found on the SU-8 passivation process. On the one hand and as demonstrated for the liquid phase analysis, a high SU-8 thickness, i.e. 3 μm and more, is responsible for a correct step coverage of the different metallic layers and, consequently, for good electrochemical properties and well-controlled active area of the related microelectrodes. On the other hand, a low SU-8 thickness, i.e. 1.6 μm or less, is still required for obtaining a low microelectrode recess and, finally, to provide the necessary electrical contact with the skin hydrolipidic film. This has to be further studied in the frame of wafer-level passivation processes (based on SU-8 polymers and/or others biocompatible materials).

References

[1] R. Feeney, S.P. Kounaves, Microfabrication of ultramicroelectrode arrays: developments, advances and applications in environmental analysis, Electroanalysis 12 (2000) 677–684.
[2] J. Castillo, S. Gaspar, S. Leth, M. Niculescu, A. Mortari, I. Bontidean, V. Soukharev, S.A. Dorneanu, A.D. Ryabov, E. Csöregi, Biosensors for life quality – design, development and applications, Sensors and Actuators B 102 (2004) 179–194.
[3] I.J. Allan, B. Vrana, R. Greenwood, G.A. Milles, B. Roig, C. Gonzales, A toolbox for biological and chemical monitoring requirements for the European Union's water framework directive, Talanta 69 (2006) 302–322.
[4] C. Spegel, A. Heiskanen, L.H.D. Skjolding, J. Emneus, Chip based electroanalytical systems for cell analysis, Electroanalysis 20 (2008) 680–702.
[5] I.E. Tothill, Biosensors for cancer marker diagnosis, Seminars in Cell & Developmental Biology 20 (2009) 55–62.
[6] S.A. Wring, J.P. Hart, Chemically modified, carbon-based electrodes and their application as electrochemical sensors for the analysis of biologically important compounds: a review, Analyst 117 (1992) 1215–1229.
[7] S. Lashi, M. Mascini, Planar electrochemical sensors for biomedical applications, Medical Engineering and Physics 28 (2006) 934–943.
[8] J. Wang, Analytical Electrochemistry, third edition, John Wiley & Sons, Inc, Hoboken, 2006.
[9] R. Kohen, Skin antioxidants: their role in aging and in oxidative stress, new approaches for their evaluation, Biomedical Pharmacotherapy 53 (1999) 181–192.
[10] C.S. Sander, H. Chang, F. Hamm, P. Elsner, J.J. Thiele, Role of oxidative stress and the antioxidant network in coetaneous carcinogenesis, International Journal of Dermatology 43 (2004) 326–335.
[11] S. Arbault, N. Sojic, D. Bruce, C. Amatore, A. Sarasin, M. Vuillaume, Oxidative stress in cancer prone xeroderma pigmentosum fibroblasts: real-time and single cell monitoring of superoxide and nitric oxide production with microelectrodes, Carcinogenesis 25 (2004) 509–515.
[12] D.R. Bickers, M. Athar, Oxidative stress in the pathogenesis of skin disease, Journal of Investigative Dermatology 126 (2006) 2565–2575.
[13] J.J. Thiele, L. Packer, Antioxidants defense systems in skin, Journal of Toxicology: Cutaneous and Ocular 21 (2002) 119–160.
[14] A. Ruffien-Ciszak, P. Gros, M. Comtat, A.M. Schmitt, E. Questel, C. Casas, D. Redoules, Exploration of the global antioxidant capacity of the stratum corneum by cyclic voltammetry, Journal of Pharmaceutical and Biomedical Analysis 40 (2006) 162–167.
[15] A.M. Bonastre, P.N. Bartlett, Electrodeposition of PANI films on platinum needle type microelectrodes. Application to the oxidation of ascorbate in human plasma, Analytica Chimica Acta 676 (2010) 1–8.
[16] F. Sekli Belaidi, P. Temple-Boyer, P. Gros, Voltammetric microsensor using PEDOT modified gold electrode for the simultaneous assay of ascorbic and uric acids, Journal of Electroanalytical Chemistry 647 (2010) 159–168.
[17] X. Xu, S. Zhang, H. Chen, J. Kong, Integration of electrochemistry in micro-total analysis systems for biochemical assays: recent developments, Talanta 80 (2009) 8–18.
[18] G.C. Fiaccabrino, M. Koudelka-Hep., Thin-film microfabrication of electrochemical transducers, Electroanalysis 10 (1998) 217–222.
[19] J.W. Schultze, V. Tsakova, Electrochemical microsystem technologies: from fundamental research to technical systems, Electrochimica Acta 44 (1999) 3605–3627.
[20] K. Stulik, C. Amatore, K. Kolub, V. Marecek, W. Kutner, Microelectrodes: definitions, characterization and applications, Pure and Applied Chemistry 72 (2000) 1483–1492.
[21] H. Suzuki, Advances in the microfabrication of electrochemical sensors and systems, Electroanalysis 12 (2000) 703–715.
[22] B. Lakard, J.C. Jeannot, M. Spajer, G. Herlem, M. de Labachelerie, P. Blind, B. Fahys, Fabrication of a miniaturized cell using microsystem technologies for electrochemical applications, Electrochimica Acta 50 (2005) 1863–1869.
[23] Y.P. Chen, Y. Zhao, J. Chu, S.Y. Liu, W.W. Li, G. Liu, Y.C. Tian, Y. Xiong, H.Q. Yu, Fabrication and characterization of an innovative solid-state microelectrode, Electrochimica Acta 55 (2010) 5984–5989.
[24] A. Schwake, B. Ross, K. Camman, Chrono amperometric determination of hydrogen peroxide in swimming pool water using an ultra-microelectrode array, Sensors and Actuators B 46 (1998) 242–248.
[25] K. Morimoto, S. Upadhyay, T. Higashiyama, N. Ohgami, H. Kusakabe, J. Fukuda, H. Suzuki, Electrochemical microsystem with porous matrix packed-beds for enzyme analysis, Sensors and Actuators B 124 (2007) 477–485.
[26] M. Miyashita, N. Ito, S. Ikeda, T. Murayama, K. Oguma, J. Kimura, Development of urine glucose meter based on micro-planar amperometric biosensor and its clinical application for self-monitoring of urine glucose, Biosensors and Bioelectronics 24 (2009) 1336–1340.

[27] D. Kim, I.B. Goldberg, J.W. Judy, Microfabricated electrochemical nitrate sensor using double-potential-step chronocoulometry, Sensors and Actuators B 135 (2009) 618–624.
[28] C.O. Parker, Y.H. Lanyon, M. Manning, D.W.M. Arrigan, I.E. Tothill, Electrochemical immunochip sensor for aflatoxin M1 detection, Analytical Chemistry 81 (2009) 5291–5298.
[29] N. Triroj, M.A. Lapierre-Devlin, S.O. Kelley, R. Beresford, Microfluidic three-electrode cell array for low-current electrochemical detection, IEEE Sensors Journal 6 (2006) 1395–1402.
[30] R. Popovtzer, T. Neufeld, A. Popovtzer, I. Rivkin, R. Margalit, D. Engel, A. Nudelman, A. Raphaeli, J. Rishpon, Y. Shacham-Diamand., Electrochemical lab on a chip for high-throughput analysis of anticancer drugs efficiency, Nanomedecine: NBM 4 (2008) 121–126.
[31] N. Pereira-Rodriguez, Y. Sakai, T. Fujii, Cell-based microfluidic biochip for the electrochemical real-time monitoring of glucose and oxygen, Sensors and Actuators B 132 (2008) 608–613.
[32] R.S. Pai, K.M. Walsh, M.M. Crain, T.J. Roussel, D.J. Jackson, R.P. Baldwin, R.S. Keynton, J.F. Naber, Fully integrated three-dimensional electrodes for electrochemical detection in microchips: fabrication, characterization and applications, Analytical Chemistry 81 (2009) 4762–4769.
[33] O. Frey, P.D. van der Wal, S. Spieth, O. Brett, K. Seidl, O. Paul, P. Ruther, R. Zengerle, N.F. de Rooij, Biosensor microprobes with integrated microfluidic channels for bi-directional neurochemical detection, Journal of Neural Engineering 8 (2011) 1–9.
[34] A. Altuna, L. Menendez de la Prida, E. Bellistri, G. Gabriel, A. Guilera, J. Berganzo, R. Vila, L.J. Fernandez, SU-8 based microprobes with integrated planar electrodes for enhanced neural depth recording, Biosensors and Bioelectronics 37 (2012) 1–5.
[35] A. Saito, A theoretical study of the diffusion current at the stationary electrodes of circular and narrow band types, Review of Polarography 15 (1968) 177–187.
[36] S.J. Konopka, B. McDuffie., Diffusion coefficients of ferri- and ferro-cyanide ions in aqueous media using twin-electrode thin-layer electrochemistry, Analytical Chemistry 42 (1970) 1741–1745.
[37] J. Legrand, E. Dumont, J. Comiti, F. Fayolle, Diffusion coefficients of ferricyanide ions in polymeric solutions – comparison of different experimental methods, Electrochimica Acta 45 (2000) 1791–1803.
[38] H. Angerstein-Kozlowska, B.E. Conway, W.B.A. Sharp, The real condition of oxidized Pt electrodes: part I, Journal of Electroanalytical Chemistry 43 (1973) 9–36.
[39] B.V. Tilak, B.E. Conway, H. Angerstein-Kozlowska., The real condition of oxidized Pt electrodes: part III, Journal of Electroanalytical Chemistry 48 (1973) 1–23.
[40] J. Barber, S. Morin, B.E. Conway, Specificity of the kinetics of H_2 evolution to the structure of single-crystal Pt surfaces, Journal of Electroanalytical Chemistry 446 (1998) 125–138.
[41] H. Angerstein-Kozlowska, B.E. Conway, B. Barnett, J. Mozota, The role of ion adsorption in surface oxide formation and reduction at noble metals: general features of the surface process, Journal of Electroanalytical Chemistry 100 (1979) 417–446.
[42] A. Berduque, B.Y.H. Layon, V. beni, G. Herzog, Y.E. Watson, K. Rodgers, F. Stam, J. Alderman, D.W.M. Arrigan, Voltammetric characterization of silicon-based microelectrode arrays and their application to mercury-free stripping voltammetry of copper ions, Talanta 71 (2007) 1022–1030.
[43] H. Möller, P.C. Postorius, The electrochemistry of gold-platinum alloys, Journal of Electroanalytical Chemistry 570 (2004) 243–255.
[44] S.P. Pappas, Photoinitiation of cationic and concurrent radical cationic polymerization, Process in Organic Coatings 13 (1985) 35–64.
[45] B.J. Polk, A. Stelzenmuller, G. Mijares, W. Mac Crehan, M. Gaitan, Ag/AgCl microelectrodes with improved stability for microfluidics, Sensors and Actuators B 114 (2006) 239–247.
[46] M.W. Shinwari, D. Zhitomirsky, I.A. Deen, P.R. Selvaganapathy, M.J. Deen, D. Landheer, Microfabricated reference electrodes and their biosensing applications, Sensors 10 (2010) 1679–1715.
[47] A.M. Sullivan, P.A. Kohl, Electro-oxidation of ascorbic acid in an aqueous citrate buffer solution, Plating and Surface Finishing 85 (1998) 56–60.
[48] Y.C. Luo, J.S. Do, C.C. Liu, An amperometric uric acid biosensor based on modified Ir–C electrode, Biosensors and Bioelectronics 22 (2006) 482–488.
[49] Y. Zhao, J. Bai, L. Wang, X.E.P. Huang, H. Wang, L. Zhang, Simultaneous electrochemical determination of uric acid and ascorbic acid using l-cystein self-assembled gold electrode, International Journal of Electrochemical Science 1 (2006) 363–371.
[50] L. Wang, J.Y. Bai, P.F. Huang, H.J. Wang, X.W. Wu, Y.Q. Zhao, Selective determination of uric acid in the presence of ascorbic acid using a penicillamine self-assembled gold electrode, Microchimica Acta 158 (2007) 73–78.
[51] H.M. Sheu, S.C. Chao, T.W. Wong, J.Y.Y. Lee, J.C.P. Tsai, Human skin surface lipid film: an ultrastructural study and interaction with corneocytes and intercellular lipid lamellae of the stratum corneum, British Journal of Dermatology 140 (1999) 385–391.
[52] C. Pailer-Mattei, S. Nicoli, R. Pirot, R. Vargiolu, H. Zahouani, A new approach to describe the skin surface physical properties in vivo, Colloids and Surfaces B68 (2009) 200–206.
[53] R. Kohen, E. Vellaichamy, J. Hrbac, I. Gati, O. Tirosh, Quantification of the overall reactive oxygen species scavenging capacity of biological fluids and tissues, Free Radical Biology and Medicine 28 (2000) 871–879.

Biographies

C. Christophe was born on December 16, 1981. She received her Engineer's Degree in materials science from the "Institut National Polytechnique de Toulouse" (France) in 2006. She joined the "Laboratoire d'Architecture et d'Analyse des Systèmes" from the French "Centre National de la Recherche Scientifique" (LAAS-CNRS) in 2007. She is working on the development of electrochemical microsensors for chemical and biochemical detection.

F. Sékli Belaidi was born on February 22, 1980. She received her Master's Degree in process and environmental engineering from the "Institut National des Sciences Appliquées de Toulouse" (France) in 2006. She joined the "Laboratoire de Génie Chimique" (LGC) from the University of Toulouse (France) in 2007. She is working on the development of electrochemical microsensors for chemical and biochemical detection.

J. Launay was born on March 11, 1975. He received the degree in electronic engineering from the Institut National des Sciences Appliquées de Toulouse" (France) in 1998. He joined the "Laboratoire d'Architecture et d'Analyse des Systèmes" from the French "Centre National de la Recherche Scientifique" (LAAS-CNRS) in 1998 and received the PhD degree from the "Institut National des Sciences Appliquées de Toulouse" (France) in 2001. In 2002, he became lecturer at the University of Toulouse (France). His research activities include the development of electrochemical microsensors for the detection in liquid phase.

P. Gros was born in 1970. He graduated in Physical Chemistry in 1992 and received his PhD degree in Chemical Engineering in 1996 at the University Paul Sabatier in Toulouse. He is now Professor in Electroanalytical Engineering in the Chemical Engineering Laboratory (Toulouse-France). He is currently working on the development of electrochemical (bio)sensors.

E. Questel was born on October 16, 1965. He received his Engineer's Degree in molecular and supramolecular chemistry from the University of Toulouse (France) in 1992. He joined the French "Groupe de Recherche sur l'Oncogénèse, les Ultraviolets et la Pigmentation Cutanée" in 1994. In 1997, he joined the French "Laboratoire Pierre FABRE Dermocosmetique" company in Toulouse. Since 2004, he is in charge of the "Skin Photobiology department". He is working on clinical studies on healthy volunteers.

P. Temple-Boyer was born on October 25, 1966. He received his Engineer's Degree in electronic engineering from the "Ecole Supérieure d'Electricité" (Paris – France) in 1990 and his Master's Degree in microelectronics from the University of Toulouse (France) in 1992. He joined the "Laboratoire d'Architecture et d'Analyse des Systèmes" (LAAS) from the French "Centre National de la Recherche Scientifique" (CNRS) in 1992 and received the PhD degree from the "Institut National des Sciences Appliquées de Toulouse" (France) in 1995. Since then, as a CNRS researcher, he has worked at LAAS on the development of physical and chemical microsensors.